Journal of Alloys and Compounds 853 (2021) 157346

Contents lists available at ScienceDirect

Journal of Alloys and Compounds

journal homepage: http://www.elsevier.com/locate/jalcom

Experimental and theoretical delimitation of the quasi-1D Tomonaga-Luttinger-liquid regime in a spin-1 field-induced antiferromagnet

H. Fabrelli , A.P. Vieira , A. Paduan-Filho , R.S. Freitas *

Instituto de Física, Universidade de São Paulo, 05508-090, São Paulo, Brazil

ARTICLE INFO

Article history:
Received 13 August 2020
Accepted 25 September 2020
Available online 28 September 2020

Keywords:
Field-induced antiferromagnet
Low-dimensional
Tomonaga-Luttinger-liquid

ABSTRACT

Through a combination of experimental and theoretical techniques, we study the spin-1 field-induced antiferromagnet $NiCl_2{-}4SC(NH_2)_2$, (DTN). Specifically, we use magnetic susceptibility and specific heat measurements, combined with Quantum Monte-Carlo calculations to delimit the quasi-1D Tomonaga-Luttinger-liquid region just above the BEC phase diagram and extend our studies to higher temperatures, where the spin interactions become negligible. This also allows us to verify some discrepancies in the value of the single-ion anisotropy parameter D, which are not well understood yet.

1. Introduction

A physical system and all the phenomena that it presents are subject to the role of dimensionality. Different dimensions reveal different symmetries that may be broken or not, leading to striking new properties or avoiding others to be present. Examples in condensed-matter physics are the absence of some phase transitions, such as Bose-Einstein condensation (BEC) for low dimensional ($d < 3$) systems [1] and the appearance of topological rather than long-range order, as in the Berezinskii-Kosterlitz-Thouless (BKT) transition in 2D XY model [2]. Regarding 1D systems, one important feature is the fact that several models can be solved exactly, in the way that the ground state can be written explicitly or easily obtained as the solution of a system of integral equations with large applicability in the real world [3,4]. Experimental advances in the research on 1D magnetic materials stimulated theoretical approaches, leading to a remarkable development in this research area in recent years [5–9].

According to Haldane's conjecture, the linear Heisenberg antiferromagnet chain with integer spin values has an energy gap between the non-magnetic ground state and the lowest-lying excited states, while the gap vanishes in the case of half-integer spin. This conjecture has been widely confirmed and is now well-established [10]. In the presence of a single-ion easy-axis anisotropy D, the Haldane gap is reduced as D is increased, but for D larger than a critical anisotropy D_c a gap reopens [11], now associated with doubly-degenerate excitonic modes [12]. This large-D gap, as the Haldane gap, is associated with a non-magnetic ground state. However, although 1D magnetic systems, defined by interactions along a single direction, are interesting for their simplicity, real materials display small interactions between chains which may lead to long-range magnetic order or in some cases to some exotic magnetic behavior.

The spin-1 system $NiCl_2{-}4SC(NH_2)_2$, known as DTN, offers a great opportunity to study low dimensional systems. The tetragonal crystalline anisotropy with an exchange interaction along the c axis leads it to behave as a collection of spin chains and, at zero external magnetic field, the small exchange interaction between chains is not strong enough to overcome the large-D gap and produce a spontaneous long-range order in the material [13–15]. The DTN compound is a sound example of a system that, upon varying the temperature and the external magnetic field, may exhibit the physics of the large-D phase, an antiferromagnetic long-range ordered phase or a paramagnetic phase. Additionally, as in other examples of field-induced antiferromagnetic systems [16–23], the prospect of a field-induced Tomonaga-Luttinger-liquid (TLL) [24] regime in DTN was studied both theoretically [25] and by nuclear magnetic resonance (NMR) experiments [26]. Those studies have shown that, due to the interplay between the large-D gap and the interchain interactions, various signatures of TLL behavior in DTN are obscured by the occurrence of the BEC of magnons at the relevant energy scales. Nevertheless, some hints of the TLL predicted behavior are still visible in experiments with DTN [25], and a cartoon of the quasi-1D TLL region is available [26]. Also,

* Corresponding author.
E-mail address: freitas@if.usp.br (R.S. Freitas).

https://doi.org/10.1016/j.jallcom.2020.157346
0925-8388/

the existence of a crossover from 1D-fermionic to 3D-bosonic magnetic excitations in DTN was studied by magnetoacoustic measurements [27], but no complete phase diagram displaying both the field-induced BEC phase and quasi-1D regime was reported as yet.

Here we make use of a combination of experimental and theoretical techniques to delimit the quasi-1D TLL regime in DTN, just above the BEC phase, quantifying the existing cartoon. The paper is organized as follows. In Sec. II we introduce the minimum theoretical model for DTN and discuss its energy scales related to the different dimensional regimes. Sec. III summarizes the experimental and numerical methods employed, and our results from magnetization, AC magnetic susceptibility and specific heat measurements together with quantum Monte Carlo (QMC) simulations are presented in Sec. IV. Finally, our conclusions and perspectives for further studies are given in Sec. V.

2. Model

DTN is a spin-1 antiferromagnet whose behavior for sufficiently small temperature and magnetic fields is described by the Hamiltonian

$$H = J_{ab}\sum_{\boldsymbol{r},\boldsymbol{e}_{ab}} \boldsymbol{S_r}\boldsymbol{S}_{\boldsymbol{r}+\boldsymbol{e}_{ab}} + J_c\sum_{\boldsymbol{r},\boldsymbol{e}_c} \boldsymbol{S_r}\boldsymbol{S}_{\boldsymbol{r}+\boldsymbol{e}_c} + D\sum_{\boldsymbol{r}}\left(S^z_{\boldsymbol{r}}\right)^2 - g\mu_B H\sum_{\boldsymbol{r}} S^z_{\boldsymbol{r}}, \tag{1}$$

where the parameters $J_{ab}/k_B = 0.18$ K, $J_c/k_B = 2.2$ K, $D/k_B = 8.9$ K and $g = 2.2$ are fitted from thermodynamic [28], neutron scattering [29] and electron-spin resonance [30] experiments. As the anisotropy parameter D is positive and about 4 times larger than the strongest exchange couplings, the ground state of the system in the absence of a magnetic field is a non-magnetic singlet characterized by a large-D gap.

The BEC phase corresponds to a field-induced XY-antiferromagnetic ordered phase occurring below $T \sim 1$ K between the critical fields $H_{c1} = 2.1$ T and $H_{c2} = 12.6$ T (for $T = 16$ mK) [28]. Above the BEC phase, for temperatures much larger than J_{ab}/k_B, so that the interchain couplings becomes negligible in comparison with thermal fluctuations, the system becomes a collection of quasi-1D spin chains along the c axis and a magnetic 3D-to-1D crossover is expected to occur. Fig. 1 illustrates the spin correlations in DTN according to the temperature range.

For higher temperatures, i.e. when $k_BT > J_c$, an approximation to

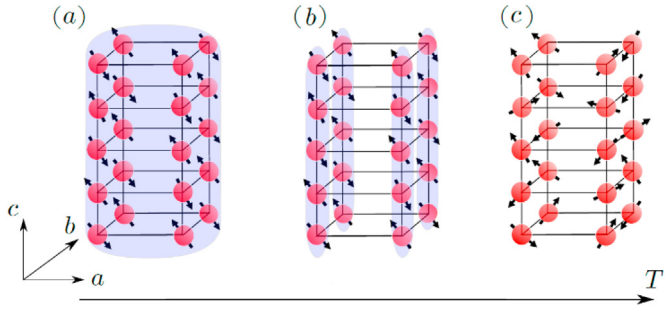

Fig. 1. Schematic representations of correlations among Ni^{2+} ions in DTN in three different regimes: (a) BEC phase, where the blue-shaded region illustrates the long-range order; (b) Quasi-1D regime, in which the interchain interaction is smaller than k_BT and the system behaves as a set of independent chains with short-range (blue-shaded) correlations; (c) quantum paramagnetic phase, where all the interactions between the sites are negligible when compared with k_BT and the spins are independent of one another. (For interpretation of the references to colour in this figure legend, the reader is referred to the Web version of this article.)

the Hamiltonian of equation (1) is given by

$$H = D\sum_{\boldsymbol{r}}\left(S^z_{\boldsymbol{r}}\right)^2 - g\mu_B H\sum_{\boldsymbol{r}} S^z_{\boldsymbol{r}}, \tag{2}$$

which is diagonal and can be written as a sum over single-ion terms with eigenvalues $E_{\pm} = D \pm g\mu BH$ and $E_0 = 0$. The partition function in this case is written simply as

$$Z = \left[1 + 2e^{-\beta D}\cosh(\beta g\mu_B H)\right]^N, \tag{3}$$

in which N is the number of magnetic lattice sites.

Since the magnetization per ion is defined as

$$M = \frac{k_BT}{N}\frac{\partial lnZ}{\partial H}, \tag{4}$$

we end up with an expression for the high-temperature magnetization in this approximation that is given by

$$M = g\mu_B\frac{sinh(\beta g\mu_B H)}{cosh(\beta g\mu_B H) + \frac{1}{2}e^{\beta D}}, \tag{5}$$

where $\beta = 1/k_BT$. Likewise, the specific heat can be calculated from

$$C = \frac{k_B\beta^2}{N}\cdot\frac{\partial^2 lnZ}{\partial\beta^2}, \tag{6}$$

with Z given by equation (3).

3. Methods

Well oriented single crystalline DTN samples were produced using the method of supersaturated solution in an aqueous medium. Measurements of AC magnetic susceptibility were performed using a 155 Hz excitation field with an amplitude of 10 Oe, through the mutual inductance bridge method in a ^{3}He cryostat with a 20 T superconductor magnet, applying the external magnetic field along the c axis. At such low frequency, AC and static susceptibility measurements are expected to be indistinguishable. Magnetization measurements and specific heat data were collected using a Quantum Design PPMS system for temperatures down to 1.8 K and under external magnetic fields of up to 9 T. Measurements of the specific heat as a function of the applied magnetic field in a nearly constant temperature were obtained using very small heat pulses, resulting in a temperature change of the sample of less than 0.04 K during the measurements.

In addition to the experimental results we performed a numerical investigation of the DTN Hamiltonian, both in its 3D version as well as in the 1D approximation, corresponding to taking $J_{ab} = 0$ in equation (1), employing the ALPS project [31] implementation of the Quantum Monte-Carlo simulations based on the directed loop algorithm in the stochastic series expansion representation [32]. For the 1D model, we simulate a chain with 256 spins, where the first 4×10^5 QMC steps were discarded to allow thermalization and using 8×10^6 steps in the calculations. In 3D simulations an $8 \times 8 \times 32$ grid was employed, discarding the first 2×10^5 and then taking the next 4×10^6. In both cases we considered periodic boundary conditions and adopted the parameters given after equation (1).

4. Results

Quite generally, TLL theory applies to the gapless regime of strictly 1D models. Of course, the fact that real systems are mostly

quasi-1D means that, however small the interchain couplings, their effect will eventually be reflected in measurements of thermodynamic properties at sufficiently low temperature. Even when one ignores interchain couplings, spin-1 systems such as DTN are gapped at sufficiently small magnetic fields, becoming gapless when the field is increased past a critical value H_{c1}, and again gapped when the field is further increased past the saturation limit H_{c2}. Thus, if the temperature is such that interchain couplings can be ignored, one should be able to capture signatures of the intermediate-field TLL behavior in the thermodynamic properties of a quasi-1D system. In order to identify those signatures, we would ideally compare experimental data with theoretical predictions for the best available model. For spin-1 systems, a precise theoretical description at finite temperature is provided by Quantum Monte Carlo simulations. However, an approximate illustration of TLL behavior for a large-anisotropy spin-1 chain such as the "1D-DTN" model, obtained when interchain couplings are ignored, is provided by a mapping to an effective spin-1/2 XXZ chain [33].

In Fig. 2a and b we present AC magnetic susceptibility curves measured as a function of the external magnetic field, applied along the c axis, for temperatures both below the critical temperature, $T_c^{BEC} = 1.2$ K, corresponding to the observation of the BEC phase (Fig. 2a), as well as above it (Fig. 2b). We compare these curves with 1D and 3D QMC simulations.

As seen in Fig. 2a and b, the low-temperature susceptibility exhibits a nonmonotonic behavior as a function of the field H. At sufficiently low temperatures, the magnetic response is small for $H \lesssim H_{c1}$, as a consequence of the large-D gap. There is a susceptibility maximum around $H \simeq H_{c1}$, associated with the closing of the gap as the ground state changes from a singlet state ($S^z = 0$) to a band of states with $S^z = 1$. Further increasing H eventually leads to saturation and to the reopening of the energy gap, marked by a second susceptibility maximum at $H \simeq H_{c2}$. For $T < T_c^{BEC}$, the maxima of the susceptibility are cusps, marking the onset of true long-range order for intermediate fields, whereas for higher temperatures these maxima are smooth. In agreement, this same distinction between cusp-like and smooth behavior for the maxima is observed in the QMC 3D results, but QMC 1D calculations always yield smooth data, as they cannot capture 3D ordering. In contrast, Fig. 2b shows that for $T > T_c^{BEC}$ there is hardly any distinction between QMC 3D and 1D results, as expected for a quasi-1D regime in which $J_{ab} \ll k_B T$. As the temperature is further increased past $T \sim J_c/k_B$, there remains a single broad susceptibility maximum, located at a field such that $g\mu_B H \simeq D$, in agreement with equation (5).

In Fig. 2c and d we highlight the difference that exists between QMC 3D and 1D calculations at $T = 0.6$ K, where the system displays a 3D ordering. Notice the cusp-like versus smooth nature of the maxima.

We performed specific heat measurements as a function of the magnetic field, $C(H)$, for temperatures down to 1.8 K and external magnetic fields up to 9 T, shown in Fig. 3a. For the higher temperatures shown in the figure, the specific heat agrees well with the one predicted by equation (6), the maxima at higher fields signaling the overcoming of the uniaxial anisotropy which favors the state $S^z = 0$. In Fig. 3b we present curves of specific heat as a function of the temperature $C(T)$ at 6 T and 8 T. (Notice that, due to limitations of the equipment, no specific heat data is available for fields larger than 9 T, so that the region around H_{c2} cannot be investigated through that technique.)

From the results presented in Fig. 3a, we observe a decrease of $C(H)$ as H increases up to a certain value of the magnetic field,

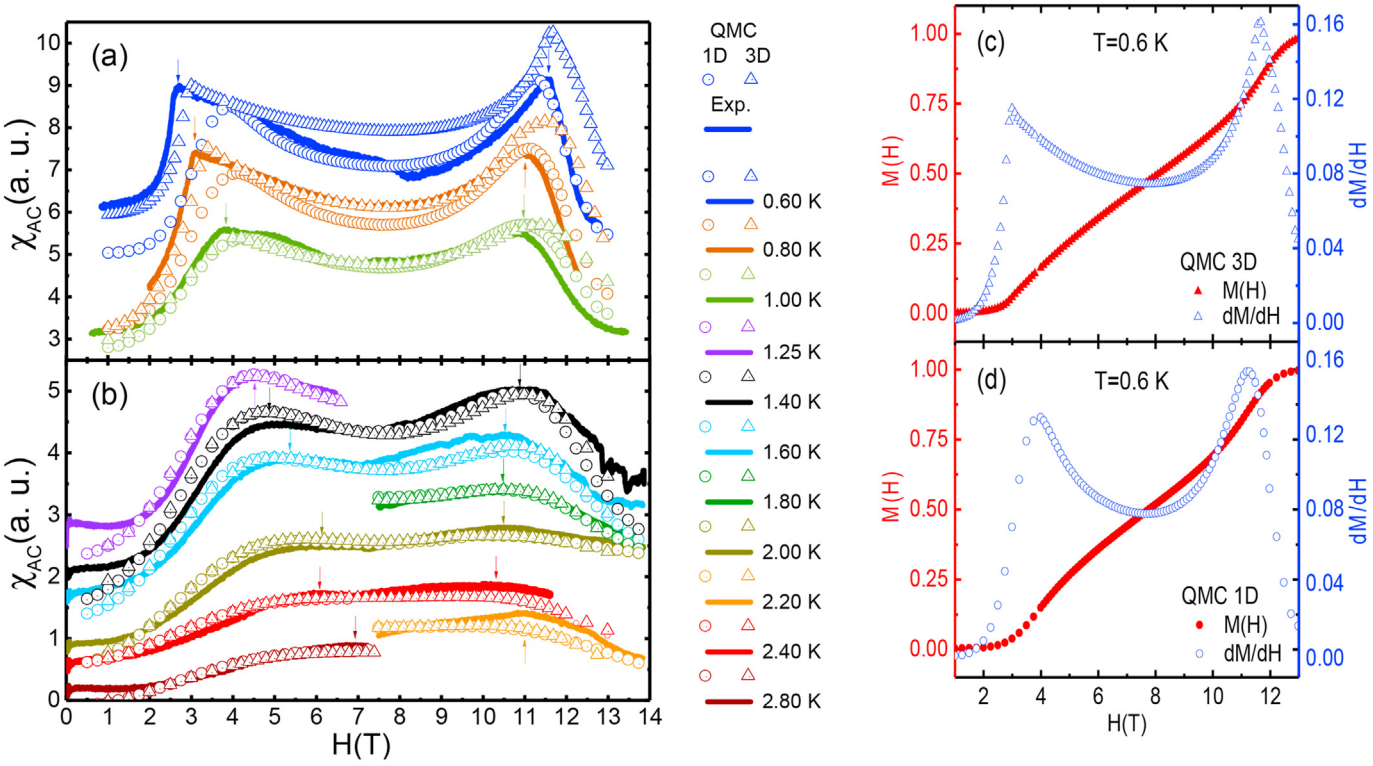

Fig. 2. (a) AC magnetic susceptibility as a function of the external magnetic field H measured at BEC regime temperatures. (b) The same as panel (a) but for temperatures above the BEC phase regime. Continuous lines correspond to our measurements while the open dots and open triangles were obtained respectively from the QMC 1D and QMC 3D calculations. The maxima of $\chi_{AC}(H)$ are indicated by arrows. All curves were shifted vertically for clarity. (c) QMC 3D and (d) QMC 1D calculations for magnetization and static susceptibility curves at $T = 0.6$ K.

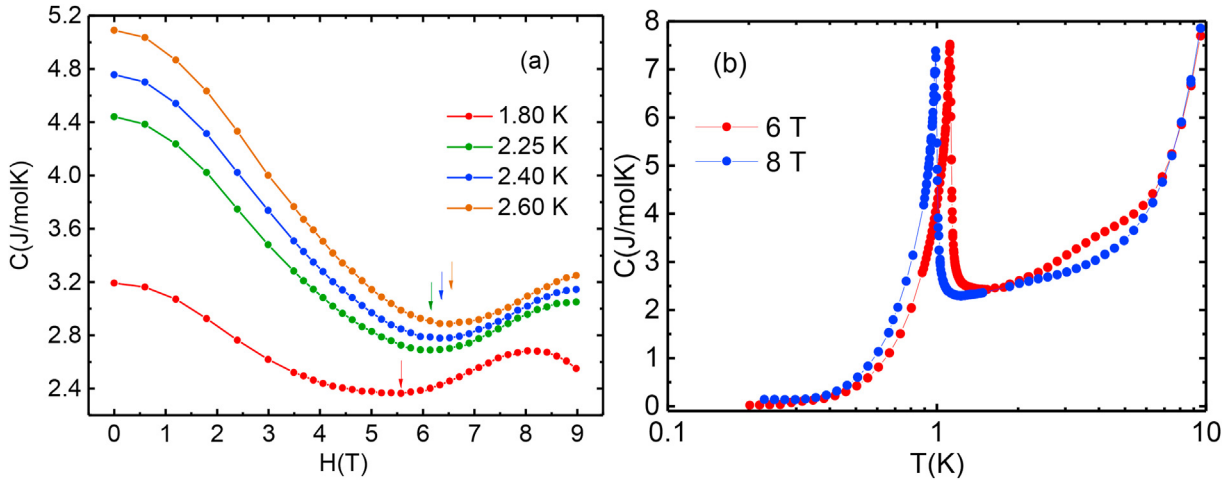

Fig. 3. Experimental data for the specific heat. (a) $C(H)$ curves for different temperatures. Arrows indicate the position of the minima of $C(H)$. (b) Specific heat as a function of the temperature, $C(T)$, at 6 T and 8 T. The narrow peaks correspond to the transition from the quasi-1D regime to the 3D ordering.

where the specific heat starts to increase again. As expected from a finite-temperature TLL regime, the minima of the specific heat are approximately located at the values of the field where the susceptibility has a maximum. We stress that these specific-heat minima and the corresponding susceptibility broad maxima do *not* indicate a phase boundary, but merely serve to signal the crossover into the TLL regime, inside which TLL theory provides a reasonable description of the thermodynamic properties. Similar results were found in a theoretical investigation of a 1D $S = 1$ chain with large easy-plane anisotropy [33], in measurements for the spin-1/2 ladder compound $(C_5H_{12}N)_2CuBr_4$ [34,35] and in optically trapped ultracold gases in a TLL regime in Ref. [36], where the authors present curves of the specific heat as a function of the chemical potential. In fact, the mapping between spin systems and Bose gases, which made possible the interpretation of the antiferromagnetic ordering in DTN and in other magnetic insulators as a BEC of magnons, relates the external magnetic field H in such systems with the chemical potential of a Bose gas [37]. This points to a connection between our results and those of ref. [36].

This correspondence between specific-heat minima and susceptibility maxima as functions of the field does not extend, of course, to a regime in which a phase transition is crossed. This is illustrated in Fig. 3b, in which the transition temperatures for two different field values are clearly associated with a narrow peak in the specific heat.

From the position of the maxima of $\chi_{AC}(H)$ and the minima of $C(H)$ we can map the region where the quasi-1D TLL regime lies in a T versus H diagram. Fig. 4 shows the well-known BEC phase diagram of DTN, obtained from previous magnetocaloric effect (MCE) and specific heat measurements (see for example ref. [29]), and the region of the TLL quasi-1D regime, obtained from our $\chi_{AC}(H)$ and $C(H)$ measurements. We compare our experimental results with 1D and 3D QMC simulations by finding the maxima of $\chi_{AC}(H)$ curves from the numerical simulations. For the TLL quasi-1D regime diagram we see that there is a good agreement between the region delimited by the experimental points and by the simulations (Fig. 2). As expected, in this region both 1D and 3D simulations nearly display the same results due to the quasi-1D nature of DTN. We call attention to the fact that the limits of the TLL quasi-1D regime in Fig. 4, as predicted by the 3D and the 1D simulations, are quite close to each other at higher temperatures, but become increasingly separated, especially at higher fields, as the temperature is reduced. Thus, effects of the interchain couplings become

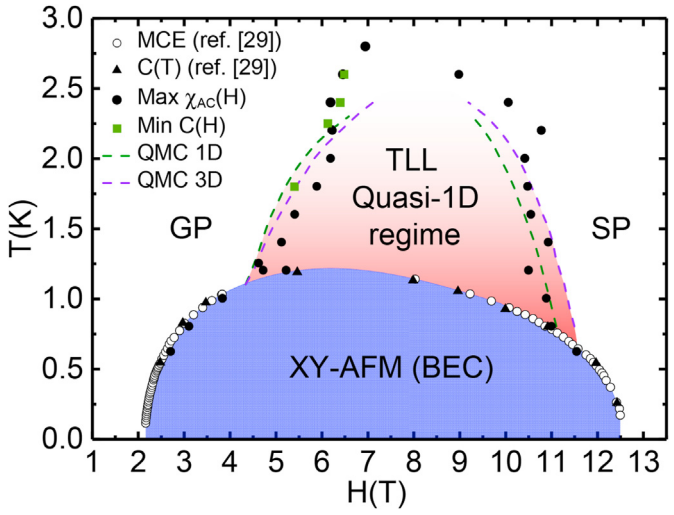

Fig. 4. BEC phase diagram of DTN (blue shaded region) from previous magnetocaloric effect (MCE) measurements and specific heat measurements (from Ref. [29]), and the TLL quasi-1D regime (red shaded region) estimated from our AC magnetic susceptibility and specific heat measurements (see text). GP stands for gapped regime while SP is the spin-polarized regime of the disordered phase. Dashed green and purple curves are obtained from the position of the maxima $\chi_{AC}(H)$ from QMC 1D and QMC 3D simulations, respectively. Notice that there are only two phases in the diagram: the XY antiferromagnetic phase in blue and the disordered region, which consists of the three different regimes indicated as GP, TLL and SP. (For interpretation of the references to colour in this figure legend, the reader is referred to the Web version of this article.)

important already in the disordered phase, signaling a crossover from 1D to 3D behavior. Some discrepancies between the experimental and simulated points may arise from the size of the grids employed in the simulations or a small misalignment of the samples.

Finally, we explore the magnetic behavior of DTN at higher temperatures, for which $k_BT > J_c$. In this regime, the major contribution to the magnetism in the system comes from the Zeeman term and the magnetocrystalline anisotropy. Fig. 5a shows the curves of DC magnetic susceptibility ($\chi_{DC}(T) \equiv M(T)/H$) in a range of temperatures from 2 K to 10 K, with an interval between two consecutive measurements of 0.03 K, and under external magnetic field up to 9 T. As the temperature decreases from 10 K, the magnetization initially increases, as in this temperature range

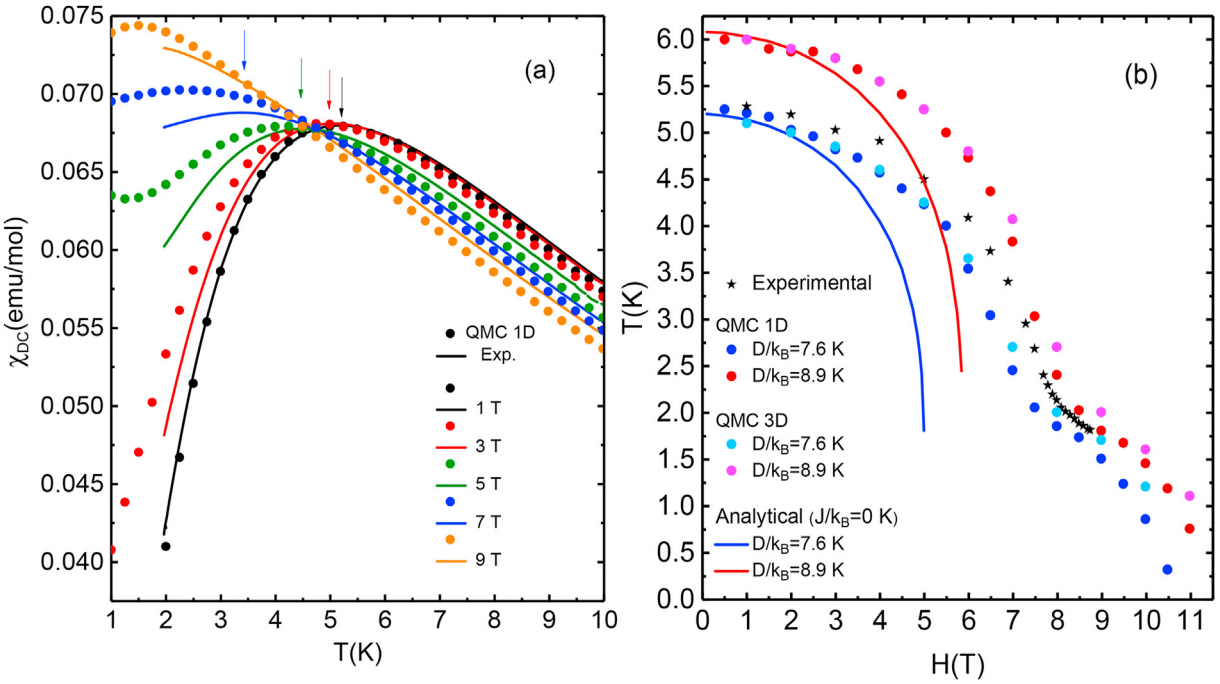

Fig. 5. (a) DC magnetic susceptibility $\chi_{DC}(T)$ curve as a function of the temperature for several external magnetic fields applied along the c axis and the comparison with QMC 1D results. Arrows indicate the position of the maxima of $\chi_{DC}(T)$. (b) Temperature of the maxima of the magnetization curves as a function of the external magnetic field. Black stars correspond to our measurements, the dots were obtained from QMC 1D calculations and the solid lines are from the analytical calculation for the magnetization taking $J_{ab} = J_c = 0$ in equation (1).

thermal energy is much higher than the pair interactions. However, at lower temperatures we observe a maximum in the magnetization curves which is associated to the short-range correlations. Increasing the external magnetic field tends to suppress these correlations, so that the higher the external magnetic field the lower the temperature in which the short-range correlations manifest themselves. This dependence of the maximum in the magnetization with the applied external magnetic field is illustrated in Fig. 5b.

When $k_BT > J_c$, an approximation to the magnetization is given by equation (5). The continuous line in Fig. 5b corresponds to the temperature of the maxima in the magnetization under several external magnetic fields. As the temperature decreases, the exchange interaction becomes relevant and the above single-ion description is no longer valid.

As shown in Fig. 5b, for low fields a good agreement between our experimental data and our theoretical results is achieved by taking $D/k_B = 7.6(4)$ K. This is significantly smaller than the value $D/k_B = 8.9$ K extracted from fits to the high-field single-magnon excitations [30]. A similar discrepancy between low-field and high-field fits to D was observed for magnon dispersion measurements in Refs. [38]. Such discrepancies may originate from other terms allowed by the crystal symmetry of DTN but not included in the Hamiltonian of equation (1). These would include, for instance, Dzyaloshinskii-Moriya interactions between Ni^{2+} ions [39] or further-neighbor interactions.

5. Conclusions

In this paper we delimited TLL quasi-1D regime lying above the 3D antiferromagnetic ordered phase in the spin-1 field-induced antiferromagnet DTN from magnetic susceptibility and specific heat measurements, corroborated by QMC calculations in 1D chains and 3D grids. Inside this TLL regime there are short-range correlations arising from the quasi-1D nature of the compound for such temperatures, since in this condition the inter-chain interactions are negligible in comparison with thermal fluctuations. Due to the magnitude of J_{ab} and the appearance of long-range order in the BEC phase, some signatures of this regime, such as a linear temperature dependence of the magnetic specific heat, are not expected to be experimentally accessible in DTN. However, the weak coupling of the spin chains can be interpreted as a weak coupling between TLL chains [22,40,41]. As usual, for higher temperatures in which both inter-chain and intra-chain interactions are much smaller than thermal fluctuations, the system displays paramagnetic behavior.

Our estimate for the single-ion anisotropy D highlights a discrepancy between the values reported in the literature based on low-field and high-field fits to experimental data, which merits further investigation. Further studies related to the present one may focus on the understanding of disorder in quasi-1D systems [42,43] including in Br-doped DTN samples and the complete understanding of the magnetic excitations in the 3D-to-1D crossover regimes, leading to interesting and complex behavior such as the crossover between fermionic and bosonic magnetic excitations.

CRediT authorship contribution statement

H. Fabrelli: Conceptualization, Resources, Investigation, Validation, Formal analysis, Writing - original draft. **A.P. Vieira:** Conceptualization, Formal analysis, Writing - review & editing. **A. Paduan-Filho:** Conceptualization, Resources, Writing - original draft, Supervision. **R.S. Freitas:** Conceptualization, Investigation, Validation, Writing - review & editing, Supervision.

Declaration of competing interest

The authors declare that they have no known competing financial interests or personal relationships that could have appeared to influence the work reported in this paper.

Acknowledgements

H. Fabrelli acknowledges financial support of National Council for Scientific and Technological Development (CNPq) (Grant No. 141629/2016-9). A. P. Vieira acknowledges the financial support of the Brazilian agencies CNPQ and São Paulo research foundation (FAPESP) (Grant No. 2017/07248−9). A. Paduan-Filho and R. S. Freitas acknowledges FAPESP (Grant No. 2015/16191−5) and CNPq (Grant No. 429511/2018−3).

References

[1] L. Pitaevskii, S. Stringari, Bose-Einstein Condensation, Clarendon Press, Oxford, UK, 2003.
[2] (a) V.L. Berezinskii, Sov. Phys. JETP 32 (3) (1971), 493;
(b) V.L. Berezinskii, Sov. Phys. JETP 34 (3) (1972), 610;
(c) J.M. Kosterlitz, D.J. Thouless, J. Phys. C Solid State Phys. 5 (L124) (1972);
(d) J.M. Kosterlitz, D.J. Thouless, J. Phys. C Solid State Phys. 6 (1181) (1973).
[3] D.C. Mattis, The Many-body Problem: an Encyclopedia of Exactly Solved Models in One Dimension, NJ World Scientific, Singapore River Edge, 1993.
[4] T. Giamarchi, Quantum Physics in One Dimension, Clarendon Press, Oxford, UK, 2003.
[5] A. Vasiliev, O. Volkova, E. Zvereva, M. Markina, npj Quant. Mater. 3 (2018), 18.
[6] C. Yasuda, S. Todo, K. Hukushima, F. Alet, M. Keller, M. Troyer, H. Takayama, Phys. Rev. Lett. 94 (2005), 217201.
[7] T. Knaflič, M. Klanjšek, A. Sans, P. Adler, M. Jansen, C. Felser, D. Arčon, Phys. Rev. B 91 (2015), 174419.
[8] M.N. Popova, S.A. Klimin, E.P. Chukalina, R.Z. Levitin, B.V. Mill, B.Z. Malkin, E. Antic-Fidancev, J. Alloys Compd. 380 (2004) 84.
[9] Jiawei Lin, Jun Deng, Zhongnan Guo, Erjian Cheng, Fan Sun, Ning Liu, Bianbian Wang, Shiyan Li, Wenxia Yuan, J. Alloys Compd. 793 (2019), 425.
[10] (a) F.D.M. Haldane, Phys. Lett. 93 (1983) 464;
(b) F.D.M. Haldane, Phys. Rev. Lett. 50 (1983) 1153.
[11] O. Golinelli, Th Jolicoeur, R. Lacaze, Phys. Rev. B 46 (1992) 10854.
[12] N. Papanicolaou, P. Spathis, J. Phys. Condens. Matter 1 (1989) 5555.
[13] V. Zapf, M. Jaime, C.D. Batista, Rev. Mod. Phys. 86 (2014) 563.
[14] V.S. Zapf, A review of bose-einstein condensation in Cu and Ni quantum magnets, in: U. Schollwöck, J. Richter, D.J.J. Farnell, R.F. Bishop (Eds.), Quantum Magnetism, Springer, Dordrecht, 2008.
[15] A. Paduan-Filho, R.D. Chirico, K.O. Joung, R.L. Carlin, J. Chem. Phys. 74 (7) (1981) 4103.
[16] S. Wessel, M. Olshanii, S. Haas, Phys. Rev. Lett. 87 (2001) 206407.
[17] M. Hagiwara, H. Tsujii, C.R. Rotundu, B. Andraka, Y. Takano, N. Tateiwa, T.C. Kobayashi, T. Suzuki, S. Suga, Phys. Rev. Lett. 96 (2006) 147203.
[18] B. Thielemann, et al., Phys. Rev. B 79 (2009), 020408(R).
[19] B. Willenberg, et al., Phys. Rev. B 91 (2015), 060407(R).
[20] M. Jeong, et al., Phys. Rev. Lett. 117 (2016) 106402. 정민기.
[21] T. Matsushita, N. Hori, S. Takata, N. Wada, N. Amaya, Y. Hosokoshi, Phys. Rev. B 95 (2017), 020408(R).
[22] M. Klanjšek, et al., Phys. Rev. Lett. 101 (2008) 137207.
[23] M. Orendáč, E. Čižmár, A. Orendáčová, J. Tkáčová, J. Kuchár, J. Černák, J. Alloys Compd. 586 (2014) 34.
[24] (a) S. Tomonaga, Prog. Theor. Phys. 5 (1950) 544;
(b) J.M. Luttinger, J. Math Phys 4 (1963) 1154;
(c) D.C. Mattis, E.H. Lieb, J. Math. Phys. 6 (1965) 304.
[25] M. Dupont, S. Capponi, N. Laflorencie, Phys. Rev. B 94 (2016) 144409.
[26] S. Mukhopadhyay, et al., Phys. Rev. Lett. 109 (2012) 177206.
[27] (a) O. Chiatti, A. Sytcheva, J. Wosnitza, S. Zherlitsyn, A.A. Zvyagin, V.S. Zapf, M. Jaime, A. Paduan-Filho, Phys. Rev. B 78 (2008), 094406;
(b) S. Zherlitsyn, O. Chiatti, A. Sytcheva, J. Wosnitza, A.A. Zvyagin, V.S. Zapf, M. Jaime, A. Paduan-Filho, J. Phys. Conf. Ser 145 (2009), 012069.
[28] A. Paduan-Filho, X. Gratens, N.F. Oliveira Jr., Phys. Rev. B 69 (2004), 020405(R).
[29] V.S. Zapf, D. Zocco, B.R. Hansen, M. Jaime, N. Harrison, C.D. Batista, M. Kenzelmann, C. Niedermayer, A. Lacerda, A. Paduan-Filho, Phys. Rev. Lett. 96 (2006), 077204.
[30] S.A. Zvyagin, J. Wosnitza, C.D. Batista, M. Tsukamoto, N. Kawashima, J. Krzystek, V.S. Zapf, M. Jaime, N.F. Oliveira Jr., A. Paduan-Filho, Phys. Rev. Lett. 98 (2007), 047205.
[31] http://alps.comp-phys.org.
[32] A.W. Sandvik, R.R.P. Singh, D.K. Campbell, Phys. Rev. B 56 (1997) 14510.
[33] C. Psaroudaki, J. Herbrych, J. Karadamoglou, P. Prelovšek, X. Zotos, N. Papanicolaou, Phys. Rev. B 89 (2014) 224418.
[34] Ch Rüegg, et al., Phys. Rev. Lett. 101 (2008) 247202.
[35] A.V. Sologubenko, T. Lorenz, J.A. Mydosh, B. Thielemann, H.M. Rønnow, Ch Rüegg, K.W. Krämer, Phys. Rev. B 80 (R) (2009) 220411.
[36] Bing Yang, Yang-Yang Chen, Yong-Guang Zheng, Hui Sun, Han-Ning Dai, Xi-Wen Guan, Zhen-Sheng Yuan, Jian-Wei Pan, Phys. Rev. Lett. 119 (2017) 165701.
[37] (a) T. Matsubara, H. Matsuda, Prog. Theor. Phys. 16 (1956) 569;
(b) É.G. Batyev, L.S. Braginskii, Sov. Phys. JETP 60 (4) (1984) 781.
[38] C. Psaroudaki, S.A. Zvyagin, J. Krzystek, A. Paduan-Filho, X. Zotos, N. Papanicolaou, Phys. Rev. B 85 (2012), 014412.
[39] S.A. Zvyagin, J. Wosnitza, A.K. Kolezhuk, V.S. Zapf, M. Jaime, A. Paduan-Filho, V.N. Glazkov, S.S. Sosin, A.I. Smirnov, Phys. Rev. B 77 (2008), 092413.
[40] T. Giamarchi, A.M. Tsvelik, Phys. Rev. B 59 (1999) 11398.
[41] H.J. Schulz, Coupled luttinger liquids, in: T. Martin, G. Montambaux, J. Trân Thanh Vân (Eds.), Correlated Fermions and Transport in Mesoscopic Systems: Proceedings of the XXXIst Rencontres de Moriond, Editions Frontieres, France, 1996.
[42] E. Altman, Y. Kafri, A. Polkovnikov, G. Rafael, Phys. Rev. Lett. 93 (2004) 150402.
[43] A. Croy, P. Cain, M. Schreiber, Eur. Phys. J. B 82 (2011) 107.